

High Performance Rh₂P Electrocatalyst for Efficient Water Splitting

Haohong Duan,^{†,‡,▽} Dongguo Li,^{§,▽} Yan Tang,^{||,▽} Yang He,[⊥] Shufang Ji,[†] Rongyue Wang,[§]

Haifeng Lv,[§] Pietro P. Lopes,[§] Arvydas P. Paulikas,[§] Haoyi Li,^{||} Scott X. Mao,[⊥] Chongmin

Wang,[#] Nenad M. Markovic,[§] Jun Li,^{*,||} Vojislav R. Stamenkovic^{*,§} and Yadong Li^{*,†}

[†]Department of Chemistry and Collaborative Innovation Center for Nanomaterial Science and Engineering, Tsinghua University, Beijing 100084, China

[‡]Chemistry Research Laboratory, Department of Chemistry, University of Oxford, 12 Mansfield Road, Oxford, OX1 3TA, UK.

[§]Argonne National Laboratory, Materials Science Divisions, Lemont, IL 60439, United States

^{||}Department of Chemistry and Key Laboratory of Organic Optoelectronics & Molecular Engineering of Ministry of Education, Tsinghua University, Beijing 100084, China

[⊥]Department of Mechanical Engineering and Materials Science, University of Pittsburgh, Pittsburgh, PA 15261, USA

[#]Environmental Molecular Sciences Laboratory, Pacific Northwest National Laboratory, Richland, WA 99352, USA

Corresponding Authors:

*junli@tsinghua.edu.cn

*vrstamenkovic@anl.gov

*ydli@mail.tsinghua.edu.cn

[▽]H.D., D.L. and Y.T. contributed equally.

Table of Contents

1. Supplementary Figures S1-17
2. Supplementary Tables S1-5

Supplementary Figures

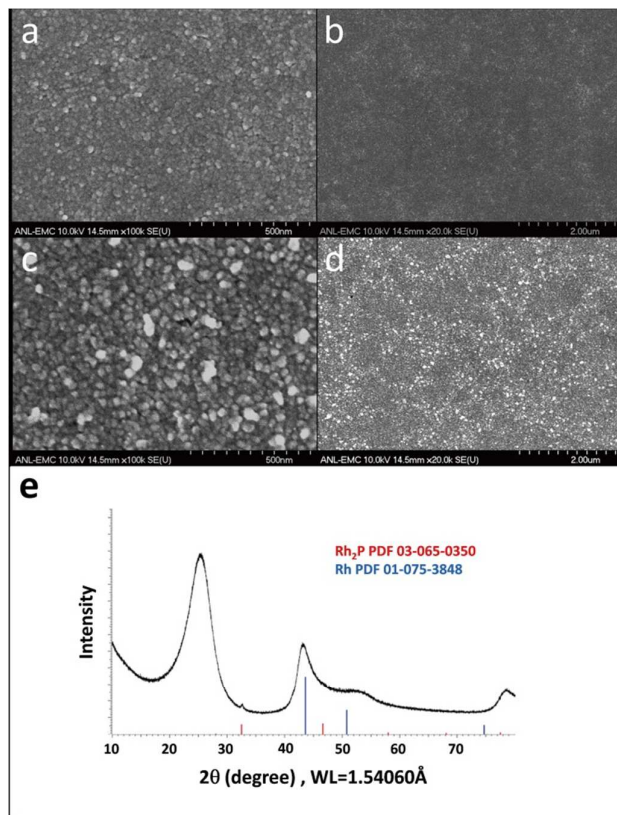


Figure S1. SEM images of the (a),(b) Rh and (c),(d) Rh₂P thin films. (e) XRD pattern of Rh₂P thin film.

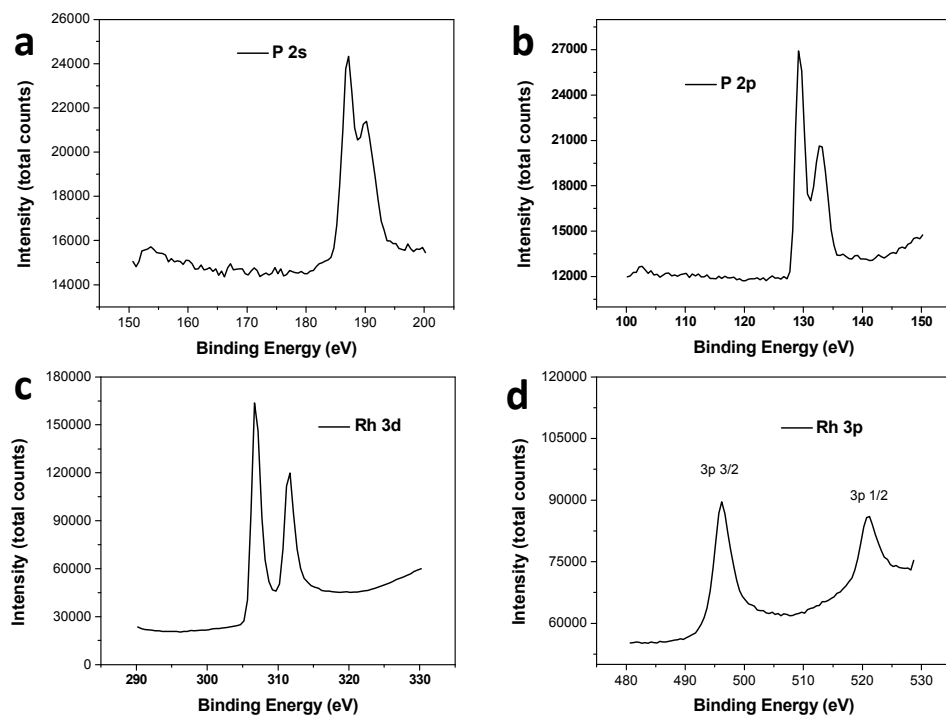


Figure S2. XPS spectra for Rh₂P thin films.* (a) Phosphorus 2s, 129.2 eV (Rh₂P), 132.7 eV (P oxide). (b) Phosphorus 2p, 187.2 eV (Rh₂P), 190.2 eV (P oxide). (c) Rhodium 3d, 306.7 eV (pure Rh), 311.7 eV (Rh₂P). (d) Rhodium 3p, 3p_{1/2}, 520.7 eV (Rh₂P), 3p_{3/2}, 496.2 eV (pure Rh). (*NIST X-ray Photoelectron Spectroscopy Database, NIST Standard Reference Database 20, Version 4.1 <https://srdata.nist.gov/xps/>)

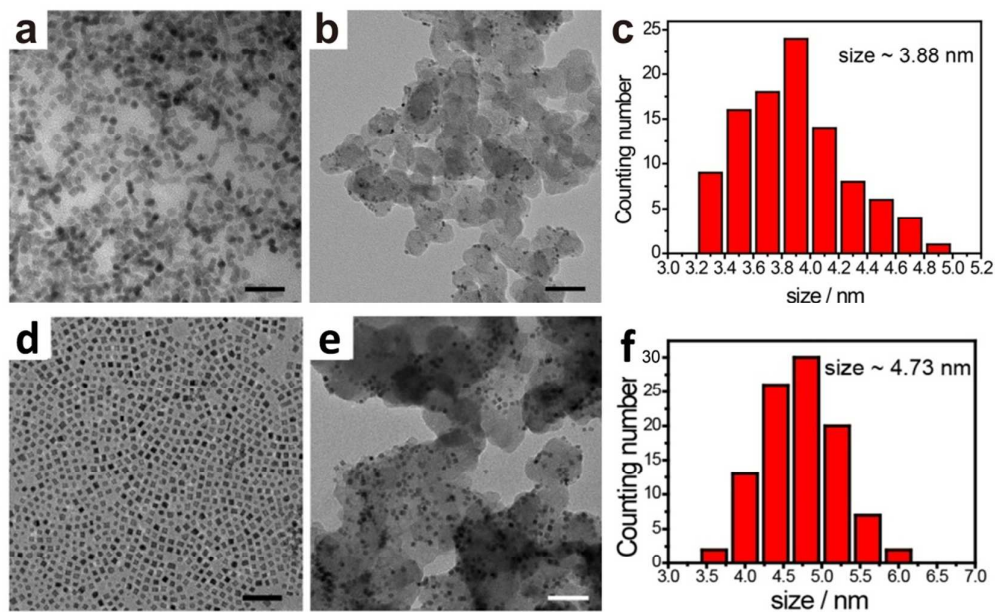


Figure S3. Characterizations of Rh NCs and Rh₂P NCs. (a-c) TEM images of as-synthesized Rh NCs (scale bar, 20 nm), Rh NCs supported on Vulcan XC-72 carbon (scale bar, 50 nm) and size distribution of Rh NCs, respectively. (d-f) TEM images of as-synthesized Rh₂P NCs, Rh₂P NCs supported on Vulcan XC-72 carbon and size distribution of Rh₂P NCs, respectively. Scale bar equals 50 nm.

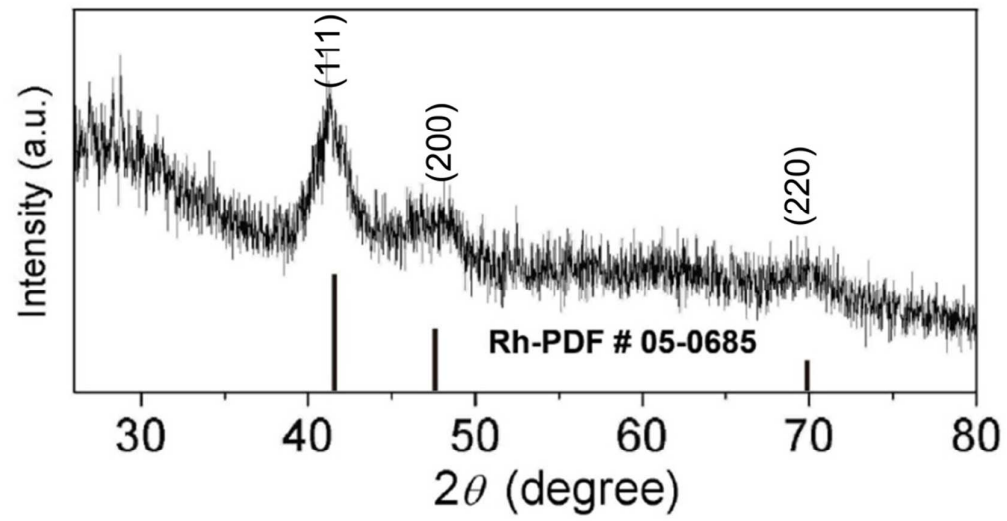


Figure S4. XRD pattern of Rh NCs. XRD pattern of Rh NCs (up) and metallic Rh (bottom, JCPDS: 05-0685).

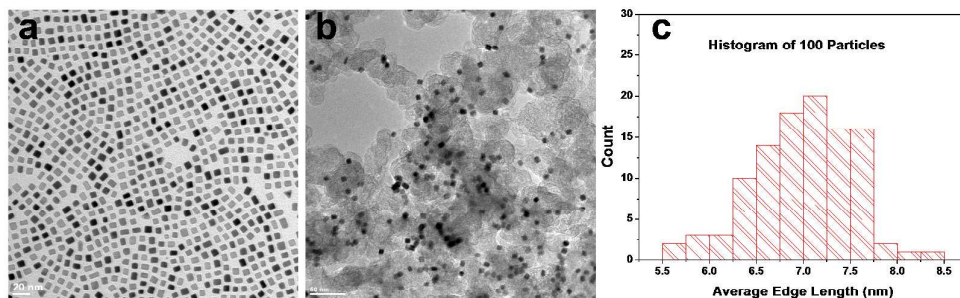


Figure S5. (a) TEM image of as-synthesized Pt nanocubes. Scale bar equals 20 nm. (b) TEM image of Pt nanocubes loaded on Vulcan XC-72 carbon after annealing at 185 °C in air. Scale bar equals 50 nm. (c) Histogram of particle size distribution counted from 100 particles. Average particle edge length is 7.0 nm \pm 0.6 nm.

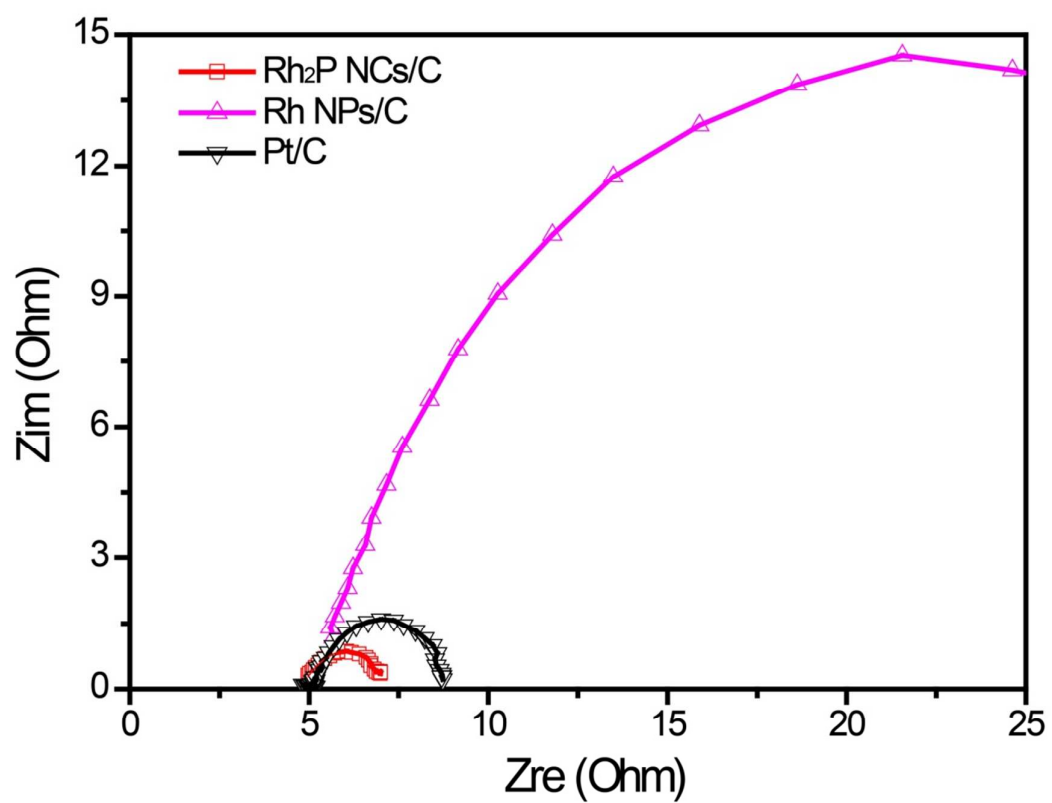


Figure S6. Nyquist plots of comparing catalysts. Nyquist plots under $\eta = 3.8$ mV.

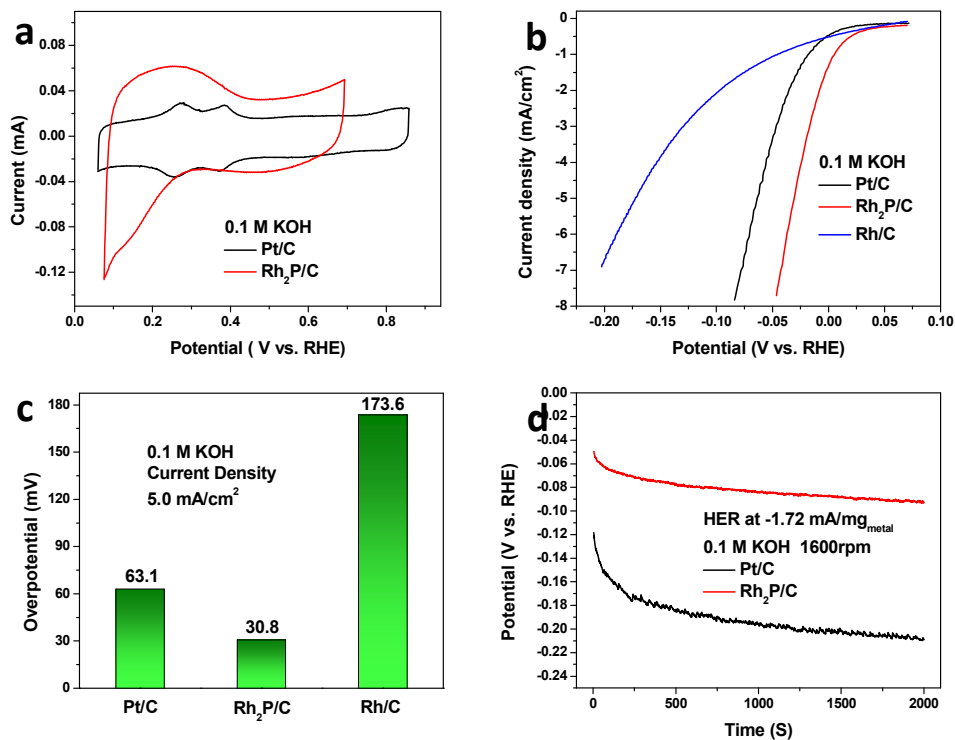


Figure S7. Hydrogen evolution reaction properties in alkaline media (0.1 M KOH). (a) Cyclic voltammograms of Rh₂P/C and Pt/C. (b) Polarization curves for Pt/C (3.7 $\mu\text{g}_{\text{Pt}}/\text{cm}^2$), Rh₂P/C (3.7 $\mu\text{g}_{\text{Rh}}/\text{cm}^2$) and Rh/C (13.3 $\mu\text{g}_{\text{Rh}}/\text{cm}^2$) recorded at 20 mV/s and (c) Corresponding overpotentials at 5.0 mA/cm² current density. (d) Chronopotentiometry of the Rh₂P/C and Pt/C recorded at -1.72 mA/mg_{metal} current density. The potentials were converted to RHE and corrected for iR drop.

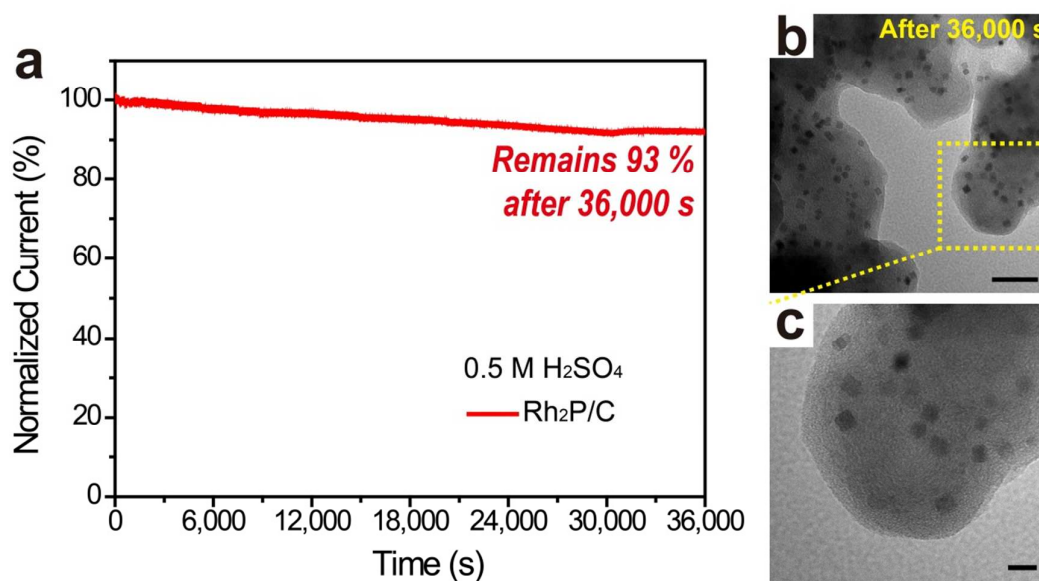


Figure S8. Durability performance of the Rh₂P catalyst. (a) Chronoamperometry for Rh₂P/C under overpotential $\eta = 109$ mV for 36,000 s, showing electrochemical durability under acidic conditions (0.5 M H₂SO₄). (b) Low-magnification (scale bar, 40 nm) and (c) high-magnification (scale bar, 10 nm) TEM images of Rh₂P/C after electrolysis for 36,000 s.

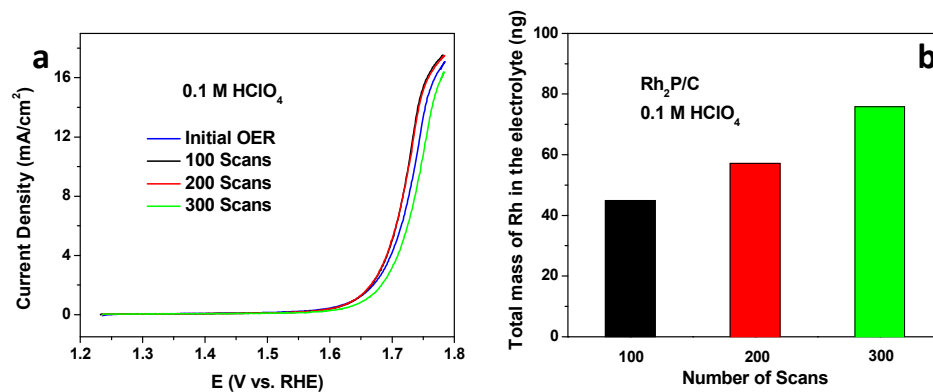


Figure S9. $\text{Rh}_2\text{P/C}$ OER stability under potential cycling. (a) Polarization curves for $\text{Rh}_2\text{P/C}$ recorded at 20 mV/s, 1600 rpm, 0.1 M perchloric acid. (b) Total mass of Rh (nanograms) in the electrolyte from ICP analysis. The potential cycling was between 1.23 V and 1.78 V, at the scan rate of 50 mV/s.

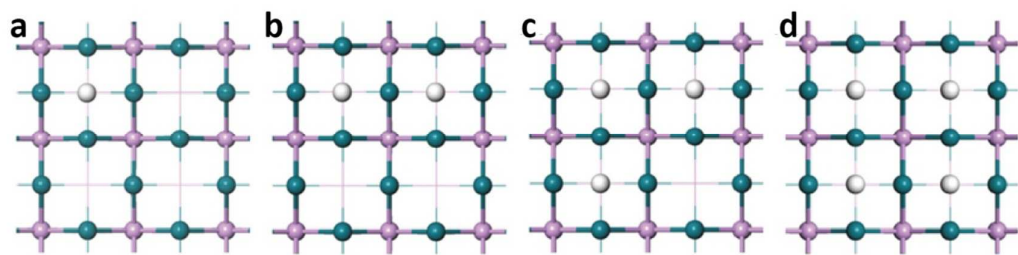


Figure S10. Optimized structures of H adsorption with different coverage on Rh-terminated surface.

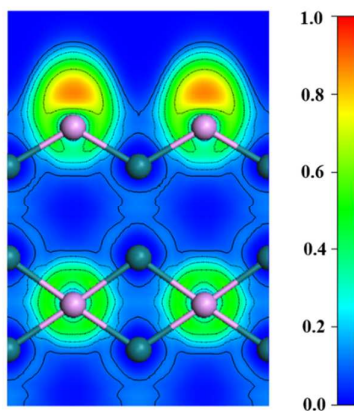


Figure S11. Calculated electron localization function (ELF) of the Rh₂P (200) surface.

The calculated ELF value ranges from 0.0 (blue) to 1.0 (red).

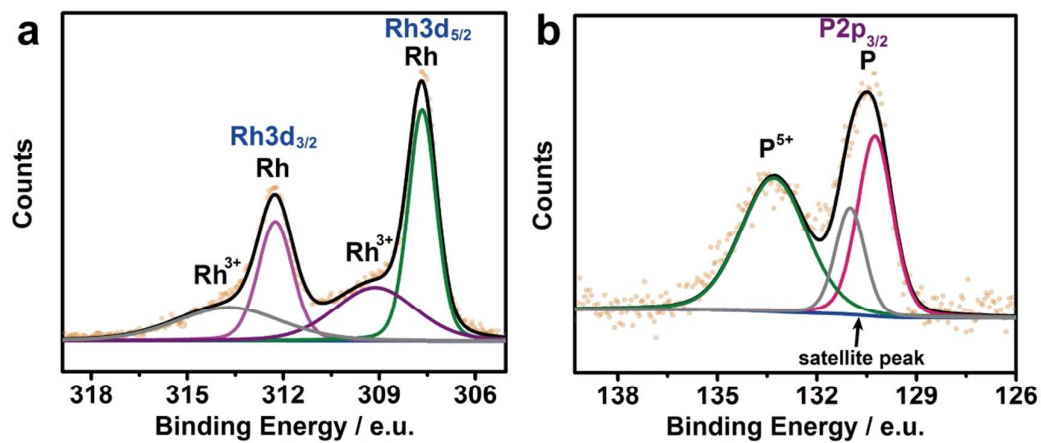


Figure S12. XPS spectra for Rh₂P/C. XPS spectra in the (a) Rh(3d) regions and (b) P(2p) region of AA washed Rh₂P/C.

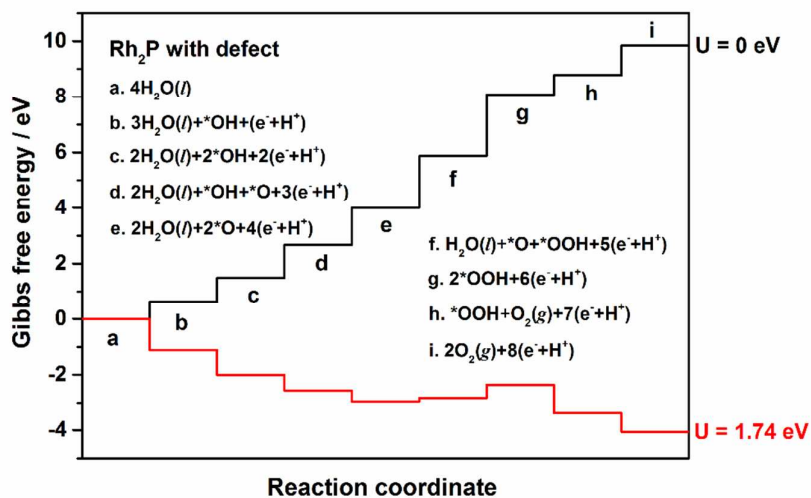


Figure S13. Gibbs free energy profiles. The calculated Gibbs free energy profiles of the intermediate states in OER on Rh₂P (200)-defect surface.

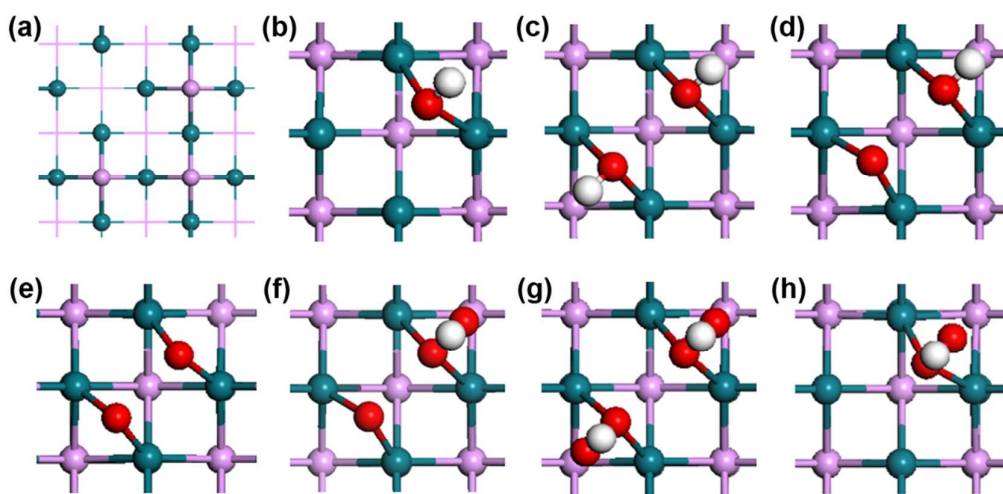


Figure S14. Optimized structures of the intermediate states in OER on Rh_2P (200)-defect surface. (a) Optimized structures of the Rh_2P (200) surface with defect. (b-h) Optimized structures of the intermediate states in OER on Rh_2P (200)-defect surface.

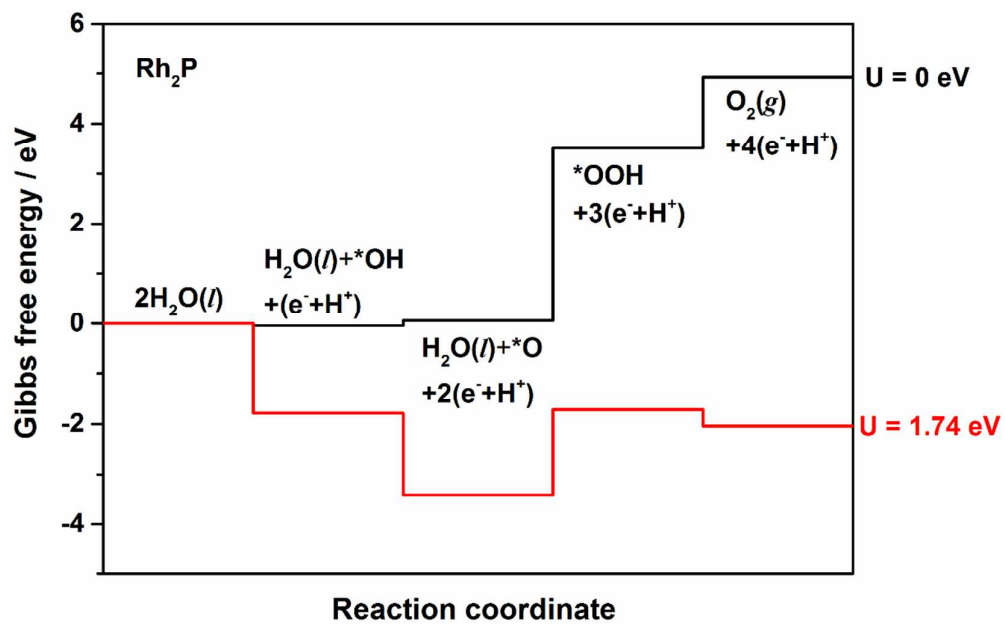


Figure S15. Gibbs free energy profiles. The calculated Gibbs free energies (eV) profiles of the intermediate states in OER on Rh_2P (200) surface.

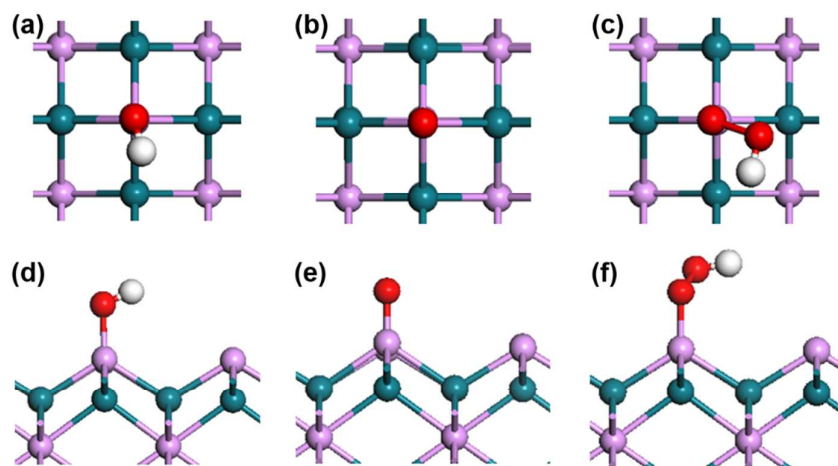


Figure S16. Optimized structures of the intermediate states in OER on Rh₂P (200) surface. (a) and (d) are the top view and side view of the *OH; (b) and (e) are the top view and side view of the *O; (c) and (f) are the top view and side view of the *OOH.

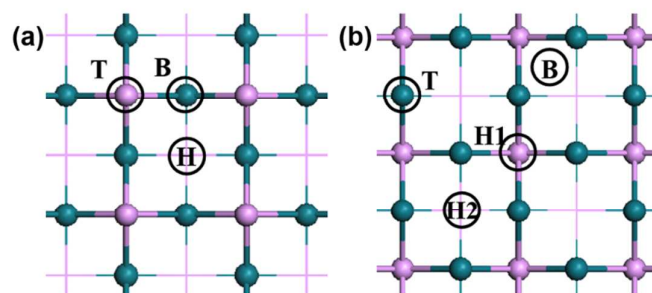


Figure S17. Binding sites of H atom. The binding sites for H adsorption on the top view of (a) P-terminated and (b) Rh-terminated Rh_2P (200) surfaces.

Supplementary Tables

Table S1. ICP-AES analysis.

Materials	Rh (μg/mL)	P (μg/mL)	Rh / P (mmol/mmol)
Rh ₂ P NCs/C (not treated by AA)	136.7	24.9	1.65
Rh ₂ P NCs ¹ /C	132.9	18.6	2.15

¹The materials were washed with AA by using method described in experimental section.

Table S2. Calculated adsorption energies and Gibbs free energies of H adsorption on Rh₂P (200) surfaces.

H coverage	P-terminated		Rh-terminated	
	ΔE_{H} (eV)	$\Delta G^{\circ}_{\text{H}}$ (eV)	ΔE_{H} (eV)	$\Delta G^{\circ}_{\text{H}}$ (eV)
1/4 ML	-0.08	0.15	-0.58	-0.51
2/4 ML	-0.25	0.00	-0.66	-0.51
3/4 ML	-0.05	0.18	-0.84	-0.66
4/4 ML	-0.06	0.17	-0.90	-0.75

Table S3. Calculated Free Energies of Reaction Steps in OER on Rh₂P (200)-defect Surface.

steps	ΔE	$\Delta_{0 \rightarrow 298K} \Delta H^{ab}$	ΔZPE	$-T\Delta S^{bc}$	$- e U$	ΔG
$H_2O \rightarrow *OH + e^- + H^+$	0.29	-0.06	-0.08	0.47	-1.74	-1.12
$H_2O \rightarrow *OH + e^- + H^+$	0.50	-0.06	-0.06	0.47	-1.74	-0.89
$*OH \rightarrow *O + e^- + H^+$	1.52	0.04	-0.17	-0.2	-1.74	-0.55
$*OH \rightarrow *O + e^- + H^+$	1.67	0.04	-0.18	-0.2	-1.74	-0.41
$H_2O + *O \rightarrow *OOH + e^- + H^+$	1.52	-0.06	-0.06	0.47	-1.74	0.13
$H_2O + *O \rightarrow *OOH + e^- + H^+$	1.87	-0.06	-0.08	0.47	-1.74	0.47
$*OOH \rightarrow O_2 + e^- + H^+$	1.61	0.13	-0.21	-0.83	-1.74	-1.03
$*OOH \rightarrow O_2 + e^- + H^+$	1.95	0.13	-0.19	-0.83	-1.74	-0.68

- a. $\Delta_{0 \rightarrow 298K} \Delta H$ denotes the correction of ΔH from 0K to 298K.
- b. These data were cited from D.R. Stull, H. Propser, JANAF Thermochemical Tables, U. S. National Bureau of Standards, Washington, DC, 1971.
- c. The value of $T\Delta S$ (H₂O) includes the correction of ΔG (H₂O) from gas to liquid.

Table S4. Calculated Free Energies of Reaction Steps in OER on Rh₂P (200) Surface.

steps	ΔE	$\Delta_{0 \rightarrow 298K} \Delta H$	ΔZPE	$-T\Delta S$	$- e U$	ΔG
$H_2O \rightarrow *OH + e^- + H^+$	-0.36	-0.06	-0.09	0.47	-1.74	-1.78
$*OH \rightarrow O^* + e^- + H^+$	0.39	0.04	-0.13	-0.2	-1.74	-1.64
$H_2O + *O \rightarrow *OOH + e^- + H^+$	3.14	-0.06	-0.10	0.47	-1.74	1.71
$*OOH \rightarrow O_2 + e^- + H^+$	3.46	0.14	-0.19	-0.83	-1.74	-0.33

Table S5. Calculated binding energies (eV) of one H atom on Rh₂P (200) surfaces

Binding site	Binding energy (eV)	
	P-terminated	Rh-terminated
top (T)	-0.07	-0.21
bridge (B)	0.63	-b
hollow1 (H1)	0.78 ^a	-c
hollow2 (H2)	0.78 ^a	-0.58

a For P-terminated Rh₂P (200) surface, hollow1 and hollow2 site are the same

b The adsorption on the bridge site is unstable and the H atom moves to the hollow2 site

c The adsorption on the hollow1 site is unstable and the H atom moves to the hollow2 site